INSTITUTE OF PHYSICS PUBLISHING SUPERCONDUCTOR SCIENCE AND TECHNOLOGY

Supercond. Sci. Technol. **16** (2003) 1026–1030 PII: S0953-2048(03)62218-9

Critical current versus strain research at the University of Twente

H J N van Eck, D C van der Laan, M Dhallé, B ten Haken and H H J ten Kate

Low Temperature Division, Faculty of Science and Technology, University of Twente, PO Box 217, 7500 AE Enschede, The Netherlands

E-mail: h.j.n.vaneck@utwente.nl

Received 8 April 2003, in final form 1 July 2003
Published 4 August 2003
Online at stacks.iop.org/SUST/16/1026

Abstract

At the University of Twente a U-shaped spring has been used to investigate the mechanical properties of a large variety of superconducting tapes and wires. Several mechanisms are responsible for the degradation of critical current as a function of applied strain. A change in its intrinsic parameters causes a reversible critical current dependence in Nb_3Sn. The critical current reaches a maximum at a wire-dependent tensile strain level, and decreases when this tensile strain is either released or further increased. In Bi-based tapes the critical current is virtually insensitive to tensile strain up to a sample-dependent irreversible strain limit. When this limit is exceeded, the critical current decreases steeply and irreversibly. This behaviour is attributed to microstructural damage to the filaments. This cracking of the filaments is verified by a magneto-optical strain experiment. Recent experiments suggest that in MgB_2 the degradation of critical current is caused by a change in intrinsic properties and damage to the microstructure. Magneto-optical imaging can be used to investigate the influence of applied strain on the microstructure of MgB_2, as is done successfully with Bi-based tapes. In all these conductors the thermal precompression of the filaments plays an important role. In Nb_3Sn it determines the position of the maximum and in Bi-based and MgB_2 conductors it is closely related to the irreversible strain limit.

1. Introduction

Knowledge of the variation of the critical current I_c with mechanical strain ε is often crucial to the successful application of technical superconductors. At the University of Twente, relatively simple devices are used to measure the $I_c(\varepsilon)$ dependence. A U-shaped spring was used in the past to study the mechanical behaviour of the low temperature superconductor Nb_3Sn and the high temperature superconductor $(Bi,Pb)_2Sr_2Ca_2Cu_3O_x$ (Bi,Pb(2223)). Recently, the same set-up was used to study the behaviour of the relatively new technical superconductor MgB_2 under applied strain. The mechanisms responsible for the degradation of the I_c in MgB_2 will be compared to those in Nb_3Sn and Bi-based tapes.

Although the U-shaped spring provides a versatile and reliable system to characterize the mechanical performance of technical superconductors, it has limitations with respect to the length scale of the measurements. Therefore the 'Pacman' has been developed to increase the sample length to gain more information regarding the homogeneity of the strain behaviour. An alternative *in situ* magneto-optical imaging (MOI) system for strained samples gives information on a local, micrometric scale, so that the relation between a sample's microstructure and its mechanical performance can be investigated directly.

2. U-shaped spring

The set-up to characterize the critical current I_c as a function of axial strain ε_a, magnetic field B and temperature T is shown in figure 1. A superconductor is soldered or glued to a U-shaped substrate. Strain is applied to the sample by bending the substrate. An insulator cup is used to create a He-gas environment around the sample. With the aid of

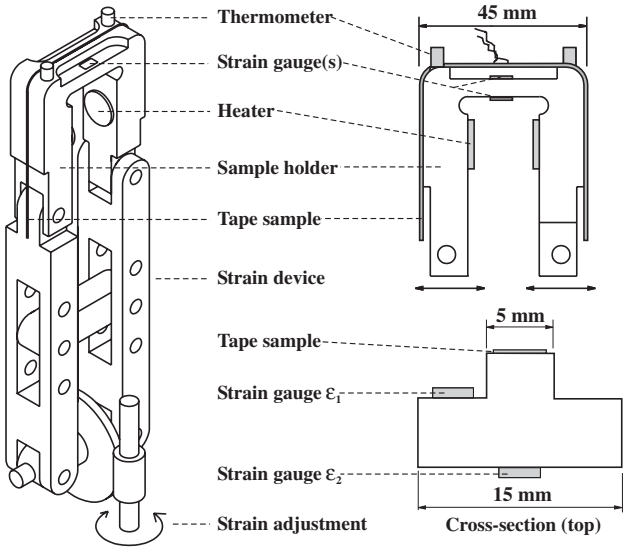

Figure 1. The U-shaped sample holder (brass, stainless steel or titanium) is deformed by a stainless steel strain device. The top part of the device can be covered by an insulator cup that enables experiments at elevated temperatures.

two thermometers and a set of heaters the sample temperature can be balanced and regulated within ±40 mK. The set-up is inserted in a solenoid magnet, with the magnetic field perpendicular to the sample.

The strain state of the superconducting filaments before the strain is applied depends on the sample reaction treatment, substrate material and fixation temperature. The first temperature change, from reaction temperature to fixation temperature, leads to a precompression of the filaments that is caused by differences in thermal contraction between the matrix material and the superconductor. In the second temperature regime, from fixation temperature to the cryogenic temperature, the substrate material determines the amount of strain inside the superconductor. Starting from the initial strain state after cool down, the substrate is bent by means of a force that acts on the legs of the U-shaped substrate. Both positive and negative strains can be applied to the sample in the range from −1% to +1%.

The strain in the sample is measured with two strain gauges that are connected to the central part of the substrate (see figure 1). The sample strain is defined as a linear function of the measured strain values (ε_1 and ε_2):

$$\varepsilon_a = A\varepsilon_1 + B\varepsilon_2 + C. \quad (1)$$

The values of the constants A and B are obtained by using a third (and temporary) strain gauge at the position of the sample. The value of C is defined at the beginning of each strain experiment by the initial condition that $\varepsilon_a = 0$, after cool down to 77 or 4.2 K. A big advantage of the use of two strain gauges is that the experiment becomes independent of a shift in the neutral line.

There are several differences when the sample is attached to a substrate compared to a free sample which is clamped at both ends:

+ homogeneous straining of the sample avoids stress concentration at weak spots;

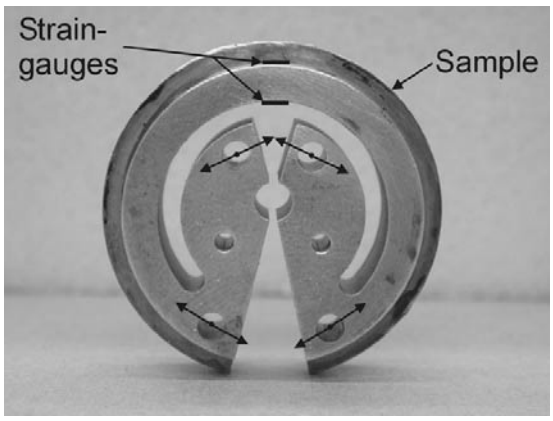

Figure 2. The Pacman. Strain is introduced in the sample by deforming the sample holder. The small dots indicate where the force is transferred to the sample holder, the arrows indicate the direction.

+ the wire can be compressed without buckling;
+ sample support for the Lorentz forces which enables accurate measurement in magnetic fields;
− no stress-free cool down possible;
− no stress measurement possible.

The limited sample length can be avoided by changing the shape of the substrate. A quite ingenious method is the Walters spring which increases the sample length to about 50 cm [1–3]. A new set-up, recently developed in our group, is the so-called Pacman (see figure 2). With this device we are able to increase the sample length up to 12 cm. Again, the sample strain is measured by two strain gauges. Just like the U-shaped spring, the set-up is equipped with two heaters and temperature sensors which enable measurements at elevated temperatures. An advantage over the Walters spring is the small size which makes it easier to regulate a homogeneous temperature.

3. Strain behaviour of Nb_3Sn and Bi-based conductors

A large number of experiments on the mechanical properties of Nb_3Sn and Bi-based conductors have been performed. In Nb_3Sn, the I_c reaches a maximum at a wire-dependent tensile strain level, and decreases reversibly when this tensile strain is either released or further increased (see figure 3). The decrease in I_c upon release of tensile strain continues reversibly when the wire is put under compression. This typical behaviour can be correlated with changes in critical temperature T_c and upper critical field B_{c2} when the crystallographic unit cell is deformed. In this sense, the mechanisms responsible for the $I_c(\varepsilon)$ dependence of A15 compounds are intrinsic in nature.

Bi-based composite superconductors display a different strain behaviour [4, 5]. Here, the I_c is virtually insensitive to tensile strain up to a sample-dependent irreversible strain limit ε_{irr}. When this limit is exceeded, I_c decreases steeply and irreversibly (see figure 4). Measurements of the magnetic field dependence of I_c at different strain levels indicate that the electrically weakly coupled grain boundaries are also the mechanically weaker ones [6, 7]. Applying compressive strain to a Bi-based tape causes a gradual and irreversible decrease of I_c. In contrast to Nb_3Sn conductors, the mechanical

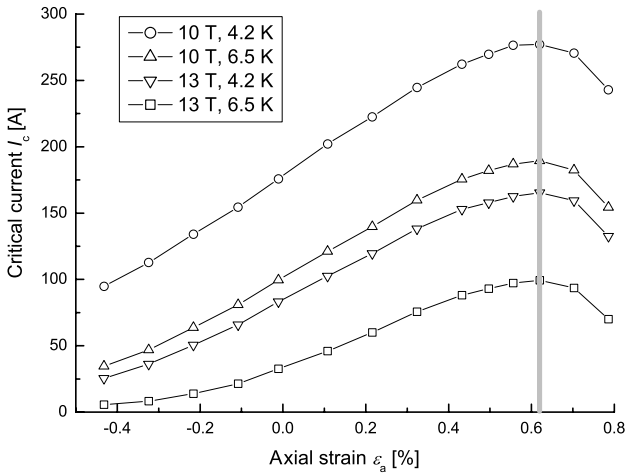

Figure 3. Critical current versus axial strain on Nb_3Sn at various fields and temperatures measured on the brass U-shaped spring. The grey bar indicates the value of thermal precompression of the superconducting filaments.

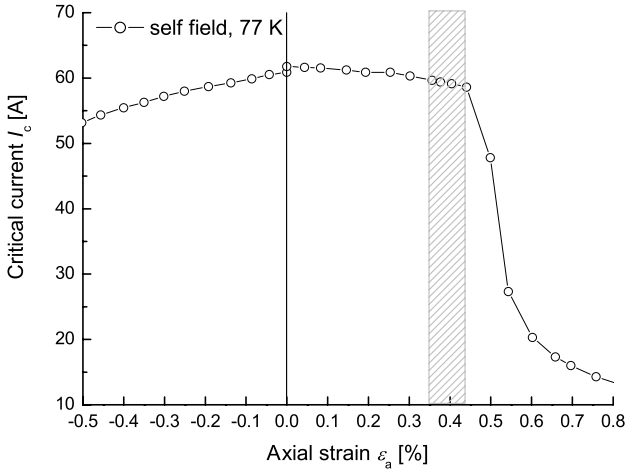

Figure 4. Critical current versus axial strain on Bi,Pb(2223) at self-field and 77 K measured on the brass U-shaped spring. The grey band indicates the approximate value of thermal precompression of the superconducting filaments.

behaviour of ceramic superconductors is understood in terms of cracking of the polycrystalline filaments and is therefore of a micromechanical nature.

In both types of conductors the thermal precompression of the superconducting filaments plays an important role. A certain amount of tensile strain needs to be applied to release the thermal precompression in order to reach a minimum in the internal strain state of the filaments. In A15 composites this precompression determines the position of the $I_c(\varepsilon)$ maximum [8]. In ceramic composite conductors it is closely related to the value of the irreversible strain limit ε_{irr} [4, 5]. As soon as the thermal precompression is released, the filaments come under tension and break when their elastic strain limit (typically $\sim$0.1% [5, 9]) is exceeded.

4. *In situ* observation of crack formation

Sørensen *et al* used scanning electron microscopy (SEM) to investigate the influence of applied strain on the microstructure

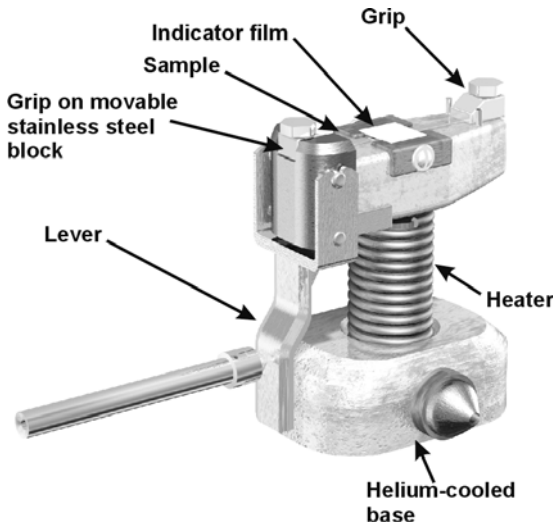

Figure 5. The MO strain device. The grips can be moved apart by means of a lever and thus straining the sample. This set-up is the property of the NHMFL in Tallahassee, FL, USA.

of Bi,Pb(2223) tapes at room temperature [9]. Their observations revealed first cracking of the filaments at a strain value of about 0.12–0.15%. The cracks continued through the complete width of the filament. The cracks zigzag through the filament which is an indication of inter-granular cracking. With increasing strain more cracks appeared.

A non-destructive tool to study the microscopic field distribution in superconducting tapes is magneto-optical imaging (MOI) [10–12]. With MOI the superconducting current paths can be made visible, which is impossible using optical or scanning microscopes.

Earlier studies [13, 14] investigated the influence of bending strain on the current paths in the filaments. The samples were bent at room temperature and subsequently cooled down to make the MO-image. However, it is not inconceivable that thermal cycling has an effect on the crack pattern. This unwanted effect can be eliminated by taking the MO-images with the strain being simultaneously applied. A set-up which enables this measurement is discussed in detail in [15]. The sample is clamped with two grips on a copper sample holder, as shown in figure 5. One of the grips is operated by a lever and can move parallel to the tape direction. An indicator film is placed on top of the sample and is held in place by two brackets. The sample is cooled by cold helium gas which flows trough the base of the holder. The sample temperature is controlled by a heater which is located around the neck of the sample holder. A copper magnet is used to apply a magnetic field up to 120 mT perpendicular to the wide side of the tape.

The resolution of MOI depends largely on the distance between the superconducting filaments and the indicator film. For this reason, a part of the sheath of the tape is removed by etching. To ensure that the etching of the silver matrix has no effect on the crack pattern, an intact sample is strained as well. The applied strain on the intact sample is measured with a strain gauge which is mounted on the sample, opposite the location of the indicator film.

The result of an experiment on a 19-filament Bi,Pb(2223) tape is shown in figure 6. The tape is zero-field cooled (ZFC) to

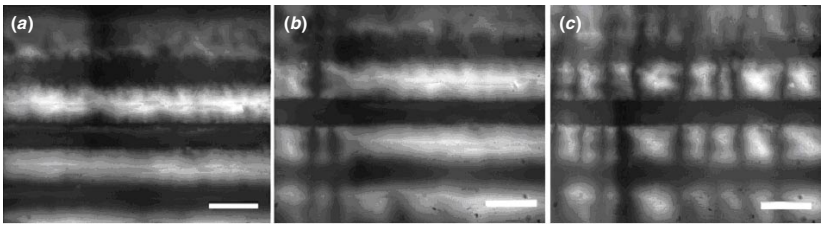

Figure 6. MO-images of an etched 19-filament Bi,Pb(2223) tape in remnant field at 30 K. In the unstrained tape (*a*), supercurrents are running along the complete length of the filaments, shielding the superconducting parts from magnetic field. When the strain is applied (*b*), cracks appear in the filaments, and interrupt the current. (*c*) Additional cracks develop in the filaments, after more strain is applied. Scale bars are 500 μm long.

30 K and subsequently exposed to an external magnetic field of 120 mT. The flux is trapped in the superconducting filaments after the external field is removed and appears bright in the picture. Dark areas indicate the absence of flux. Figure 6(*a*) shows the MO-image of the unstrained tape. The filaments run horizontally through the picture and are completely penetrated by the magnetic field. Note that only the top layer of filaments is visible.

Some detailed structures in the bright areas are visible, indicating a variation of current density inside the filament. This is an indication of the presence of either microcracks, boundaries between colonies of well-connected grains or variations in filament width and thickness. After applying tensile strain to the sample, cracks develop as can be seen in figure 6(*b*). The shielding currents are stopped at the cracks and the cracks appear dark on the MO-image. The cracks seem to propagate through the matrix into the neighbouring filaments. When the strain is further increased more cracks develop, see figure 6(*c*). In the measurement with the intact sample, the first three cracks appear at strains of 0.65%, 0.73% and 0.77%, which are higher than the value of $\varepsilon_{\rm irr}$, so the $I_{\rm c}$ is already degraded before any cracks are visible. This may be due to the fact that only the top layer of the filaments is visible in the MO-image or the development of microcracks, not visible in MOI.

Since colony boundaries are mechanically weaker it is anticipated that the filaments break at these locations. Cracks are formed in the filaments spaced about 200 μm apart. This result is in agreement with the ultrasonic fracturing experiments done by Larbalestier *et al* [16]. The distance between the cracks is an indication of the average size of colonies, consisting of well-connected grains.

5. Strain behaviour of MgB_2 conductors

Recently, MgB_2 tapes produced by the *ex situ* powder-in-tube (PIT) process (MgB_2 powder in a metal sheath) have been measured with the U-shaped spring [17]. Figure 7 shows the strain dependence of the critical current in a four-filament tape with an aspect ratio of 4. After cool down to 4.2 K tensile strain is applied. The experiment clearly shows the two distinct $I_{\rm c}(\varepsilon)$ regimes ($\varepsilon < \varepsilon_{\rm irr}$: reversible; $\varepsilon > \varepsilon_{\rm irr}$: irreversible) that are found in such tapes.

In part A $\rightarrow$ B the $I_{\rm c}$ increases linearly to a sample-dependent irreversible strain limit, after which $I_{\rm c}$ decreases

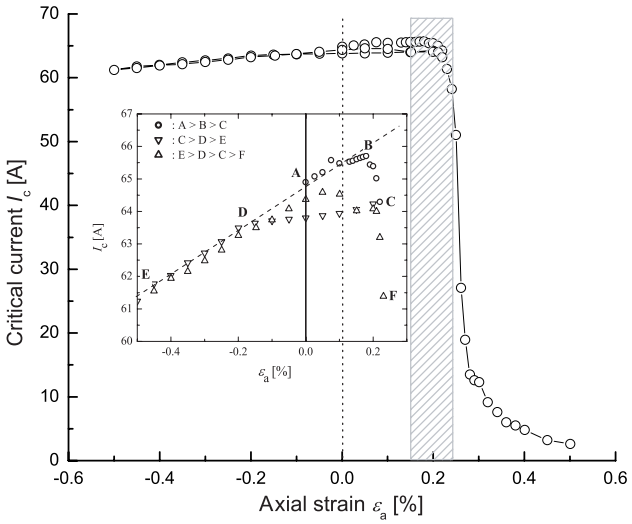

Figure 7. Critical current versus axial strain on MgB_2 at 4 T and 4.2 K measured on the titanium U-shaped spring. The grey band indicates the approximate value of thermal precompression of the superconducting filaments.

sharply. From C through D to E the tensile strain is first released and the tape is put under compression. During the part C $\rightarrow$ D $I_{\rm c}$ decreases slowly. Between D and E, however, it degrades with the same linear dependence as during the initial part A $\rightarrow$ B. We interpret this as a re-closing of the cracks that originated from the part B $\rightarrow$ C [17]. Since the damage occurring during this initial cracking is still relatively small ($\sim$2.5% of the total current) it appears that the cracks can still be pushed together to carry (within experimental uncertainty) the same current as the undamaged tape. The slope of the dashed line through E and B is roughly 8% per per cent strain but varies between 8 and 17% for other investigated samples. At E, the sweep direction of the strain is reversed. From E to D the $I_{\rm c}$ follows nearly the same linear curve, then it fluctuates from D to C and eventually, during C $\rightarrow$ F, continues the steep degradation which was started at B $\rightarrow$ C. An increase in the strain of $\Delta\varepsilon \approx 0.1\%$ is needed for $I_{\rm c}$ to degrade from 90% to 10% of its unstrained value, which is smaller than that for most Bi-based tapes.

This behaviour demonstrates several general features:

- irreversible $I_{\rm c}(\varepsilon)$ degradation for tensile strain exceeding $\varepsilon_{\rm irr}$, indicative of cracks appearing in the microstructure;
- reversible $I_{\rm c}(\varepsilon)$ dependence for compressive strains and tensile strains below $\varepsilon_{\rm irr}$;

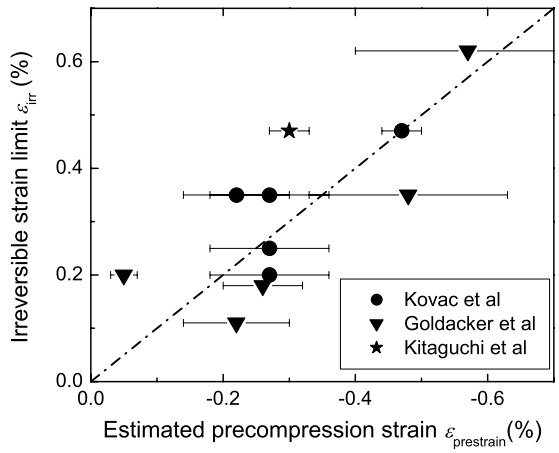

Figure 8. Measured reversible strain limits ε_{irr} of MgB_2/metal composites, plotted as a function of estimated thermal precompression strain $\varepsilon_{prestrain}$ in the filaments. The circles correspond to the MgB_2/Fe wires presented in [17], the triangles to mono-filamentary MgB_2/Fe and MgB_2/Fe/steel wires presented by Goldacker *et al* [19, 20] and the star to a mono-filamentary MgB_2/steel wire presented by Kitaguchi *et al* [18]. The dashed line indicates the relation $\varepsilon_{irr} = -\varepsilon_{prestrain}$.

- if the tape is put under compression after exceeding ε_{irr}, I_c stays constant until a reversible compressive 'master curve' is regained;
- re-application of tensile strain causes the I_c to rise again until the value by which it was degraded by tensile strain is reached.

The $I_c(\varepsilon)$ behaviour of MgB_2 seems to combine the strain mechanism behind A15 composites and ceramic superconductors; a reversible degradation for compressive strains and tensile strains below ε_{irr}, and an irreversible degradation above ε_{irr}. Again, the value of ε_{irr} seems closely related to the precompression of the filaments. We use the rule of mixtures to estimate the thermal precompression of the MgB_2 filaments after cool down to 4.2 K [17]. Also the MgB_2/metal composites presented by Kitaguchi *et al* [18] and Goldacker *et al* [19, 20] are analysed in terms of thermal prestrain.

The precompression estimates are plotted against the measured irreversible strain limits in figure 8. All data lie grouped around the line $\varepsilon_{irr} = -\varepsilon_{prestrain}$ and we can thus conclude that ε_{irr} is closely related to the level of precompression of the MgB_2 filaments. As is the case in Bi-based conductors, the filaments will not be damaged by an applied tensile strain as long as the strain does not fully compensate the compressive thermal stress.

The question arises if the reversible $I_c(\varepsilon)$ dependence under compression is related to changes in T_c or B_{c2}. In order to verify if the irreversible degradation of I_c is caused by damage to the microstructure, MOI strain experiments would be very helpful.

6. Conclusions

- Strain behaviour of Nb_3Sn can be related to changes in T_c and B_{c2}.
- Strain behaviour of Bi-based conductors is understood in terms of cracking of the ceramic filaments and is of a microstructural nature. This is supported with MOI strain experiments.
- Strain behaviour of MgB_2 is related to a change of intrinsic properties, combined with damage to the microstructure. The origin of I_c variation with strain appears to be microstructural for strains exceeding ε_{irr} and might be related to T_c and B_{c2} for strains below ε_{irr}.
- More experiments on the strain behaviour of MgB_2 will have to be carried out. These include $I_c(B, T, \varepsilon)$ to investigate the intrinsic properties and MOI strain experiments to investigate the microstructure. MOI has been used to successfully show the crack development in Bi-based tapes.

References

[1] Walters C R, Davidson I M and Tuck G E 1986 *Cryogenics* **26** 406–6
[2] Uglietti D, Seeber B, Abächerli V and Flükiger R 2002 Critical current vs. strain measurements of long length Nb_3Sn wires up to 1000 A and 17 T using a modified Walters spring *ASC 2002*
[3] Cheggour N and Hampshire D P 2000 *Rev. Sci. Instrum.* **71** 4521
[4] ten Haken B, Godeke A, Schuver H-J and ten Kate H H J 1996 *IEEE Trans. Magn.* **32** 2720–3
[5] Passerini R, Dhallé M, Giannini E, Witz G, Seeber B and Flükiger R 2002 *Physica* C **371** 173–84
[6] Huang Y K, ten Haken B and ten Kate H H J 1999 *IEEE Trans. Appl. Supercond.* **9** 2702–5
[7] Passerini R, Dhallé M, Porcar L, Marti F, Witz G, Seeber B, Grasso G and Flükiger R 1999 *Inst. Phys. Conf. Ser.* **167** 607–10
[8] Godeke A, ten Haken B and ten Kate H H J 1999 *IEEE Trans. Appl. Supercond.* **9** 161–4
[9] Sørensen B F, Horsewell A and Skov-Hansen P 2002 *Physica* C **372–376** 1032–5
[10] Indenbom M V, Nikitenko V I, Polyanskii A A and Vlasko-Vlasov V K 1990 *Cryogenics* **30** 747
[11] Indenbom M V, Kolesnikov N N, Kulakov M P, Naumenko I G, Nikitenko V I, Polyanskii A A and Vlasko-Vlasov V K 1990 *Physica* C **166** 486
[12] Koblischka M R and Wijngaarden R J 1995 *Supercond. Sci. Technol.* **8** 199
[13] Koblischka M R, Johansen T H and Bratsberg H 1997 *Supercond. Sci. Technol.* **10** 693
[14] Polak M, Parrell J A, Polyanskii A A, Pashitski A E and Larbalestier D C 1997 *Appl. Phys. Lett.* **70** 1034
[15] van der Laan D C, van Eck H J N, Davidson M W, ten Haken B, ten Kate H H J and Schwartz J 2002 *Physica* C **372–376** 1020–3
[16] Larbalestier D C *et al* 1998 New experiments elucidating the current limiting mechanisms of Ag-sheathed $Bi,Pb_2Sr_2Ca_2Cu_3O_x$ tapes *Adv. Supercond.* **11** 805–10
[17] Kovác P, Dhallé M, Melisek T, van Eck H J N, Wessel W A J, ten Haken B and Husek I 2003 *Supercond. Sci. Technol.* **16** 600–7
[18] Kitaguchi H, Kumakura H and Togano K 2001 *Physica* C **363** 198
[19] Goldacker W and Schlachter S I 2002 *Physica* C **378–81** 889
[20] Goldacker W, Schlachter S I, Reiner J, Zimmer S, Nyilas A and Kiesel H 2002 *ASC 2002*